ORIGINAL RESEARCH

Inverse opal substrate-loaded mesenchymal stem cells contribute to decreased myocardial remodeling after transplantation into acute myocardial infarction mice

Wenbin Lu[1,*]
JingJing Ji[1,*]
Genshan Ma[1]
Qiming Dai[1]
Lijuan Chen[1]
Pengfei Zuo[1]
Yuanjin Zhao[2]

[1]Department of Cardiology, ZhongDa Hospital Affiliated with Southeast University, Nanjing, China; [2]State Key Laboratory of Bioelectronics, School of Biological Science and Medical Engineering, Southeast University, Nanjing, China

*These authors contributed equally to this work

Correspondence: Wenbin Lu
Department of Cardiology, ZhongDa Hospital Affiliated with Southeast University, 87 Dingjiaqiao Road, Nanjing 210009, China
Email luwenbinseu@163.com

Yuanjin Zhao
State Key Laboratory of Bioelectronics, School of Biological Science and Medical Engineering, Southeast University, 2 Sipailou Road, Nanjing 210009, China
Email yjzhao@seu.edu.cn

Background: The two-dimensional incubation method is now the most commonly method for mesenchymal stem cell (MSC) production. however, gene expression and secretion of growth factors are relatively low; thus, the transplanted cells cannot be effectively utilized for potential clinical applications after acute myocardial infarction (AMI).

Objectives: We aimed to investigate whether our newly made substrates of inverse opal with specific surface microstructures for MSC culturing can increase the viability of the cells and can contributes to decreased myocardial remodeling after transplanted to AMI mice.

Methods: The inverse opal structure is fabricated by the convenient bottom-up approach of the self-assembly of colloidal nanoparticles. Mouse-derived MSCs were then cultured on the substrates when expanded at different times to investigate the cell growth status including morphology. Then the inverse opal substrates loaded MSCs were transplanted to AMI mice, cardiomyocyte apoptosis and LV remodeling were further compared. To explore the possible mechanisms of curation, the secretions and viability of MSCs on substrates were determined using mice ELISA kits and JC-1 mitochondrial membrane potential assay kits respectively at normal and hypoxic conditions.

Results: 6 times expanded inverse opals allowed greatly the orderly growth of MSCs as compared to four ($34\% \pm 10.6\%$) and two ($20\%\pm7.2\%$) times expanded as well as unexpanded ($13\%\pm4.1\%$) ($P<0.001$). Nearly 90% of MSCs showed orientation angle intervals of less than 30° when at the 6X expanded ($89.6\%\pm25\%$) compared to the percent of cells with 30°–60° ($8.7\%\pm2.6\%$) or $\geq$60° ($1.7\%\pm1.0\%$) orientation angle ($P<0.001$). After inverse opal loaded MSCs transplanted to AMI mice, greatly decreased apoptosis of cardiomyocytes ($20.45\%\pm8.64\%$ vs.$39.63\%\pm11.71\%$, $P<0.001$) and infarction area (5.87 ± 2.18 mm^2 vs 9.31 ± 3.11 mm^2, $P<0.001$) were identified. In the end, the viability of inverse opal loaded MSCs determined by membrane potential ($P<0.001$) and the secretion of growth factors including VEGF-α, SDF-1 and Ang-1 ($P<0.001$) were both confirmed significantly higher than that of the conventional culture in petri dish.

Conclusion: The structure of inverse opal can not only adjust the arrangement of MSCs but also contribute to its orientated growth. Inverse opal loaded MSCs transplantation extremely curbed myocardial remodeling, the underlying mechanisms might be the high viability and extremely higher secretions of growth factors of MSCs as devoted by this method.

Keywords: MSCs, inverse opal, AMI

Introduction

Acute myocardial infarction (AMI) is extremely associated with high mortality. It remains a big challenge to curb myocardial remodeling now.[1] Strategies to control

AMI-related complications and myocardial remodeling in the first several days after AMI are pivotal, for ischemic and hypoxic cardiomyocytes can still be repaired in this condition. Stem cell transplantation into the injured heart after AMI is now believed to reduce initial damage, promote activation of the regenerative potential of the heart, and integrate the regenerated tissue. Mesenchymal stem cells (MSCs) have long been used as optimal stem cells that can be transplanted after AMI.[2–5]

MSCs are usually identified by the presence of surface markers like CD73, CD90, and CD105 and absence of markers like CD14, CD34, and CD45.[6] The paracrine effects of transplanted MSCs are now considered to be the main mechanism by which they exhibit therapeutic effects, mainly due to the secretion of stromal cell-derived factor 1 (SDF-1), angiopoietin-1 (Ang-1), and vascular endothelium growth factor-α (VEGF-α).[7] Researchers have recently identified that inappropriate growth of the transplanted MSCs in vivo makes them incapable of fully secreting the required growth factors. Thus, new strategies are urgently needed to improve the cell viability of transplanted MSCs. Compared to the traditional methods of culturing MSCs, which involve two-dimensional production with relatively disorderly growth, we have been exploring new ways to enable the cells to grow in an orderly manner as well as investigating a better method to produce MSCs with improved viability and increased capacity to secrete growth factors.[8–12] Currently, most of the substrates can only increase the density of cultured cells, rather than control the orientation of cells, which is critical to cell secretion. Hence, transplanted cells cannot produce better effects after AMI. Thus, novel substrates for efficient loading of MSCs are urgently needed for optimizing the biological features of the cells.[13–16]

Here, we present a novel method for fabricating patterned substrates, which can efficiently load MSCs and contribute to an orderly alignment of the cells. Our substrate is an expanded inverse opal structure, which is derived from the convenient bottom-up approach involving the self-assembly of colloidal nanoparticles.[17–19] Based on the amount of expansion experienced by inverse opal substrates, they can result in nanoscale patterned structures with different degrees of orientation. When MSCs are seeded on the substrates having these patterned structures, both morphology and alignment of cells can be adjusted. We confirmed that the alignment of MSCs on the inverse opal substrates greatly benefited in the recovery of AMI mice and greatly increased the survival, which can be attributed to increased secretion of growth factors by MSCs in this method. This functional inverse opal substrate will be utilized in important applications where MSC transplantation is carried out for the treatment of AMI.

In conclusion, the main objective of our study was to investigate whether newly prepared substrates of inverse opal with specific surface microstructures can increase the viability of the cells and can contribute toward decreased myocardial remodeling after transplantation into AMI mice.

Materials and methods
Preparation of inverse opal substrates
Monodisperse silicon dioxide spheres with a diameter of 420 nm were first synthesized and determined with Zeta potential (mv) (Figure S1). In brief, monodisperse silica spheres (1% w/v, 420 nm; Nanjing Nanorainbow Biotechnology Co.) were dipped into an ethanol solution and deposited on glass by vertical deposition.[20–23] After 24 hours of evaporation of ethanol at room temperature, 20% polystyrene–toluene (Aladdin Reagent Co.) solution was then infiltrated into the voids of the opal template. Due to the volatile nature of toluene, the film will automatically fall off from the slide. The silica spheres were etched with 4% hydrofluoric acid and washed with demi water for 6 hours to form a free-standing inverse opal film. Then, inverse opal substrates were expanded to different degrees, approximately one, two, four, and six ×, at 75°C using a Vernier caliper (Masterproof, Hannover, Germany). Inverse opal substrates were first immersed in 75% ethanol solution overnight in the presence of ultraviolet light. Then, they were washed three times with sterile PBS solution, and the inverse opal substrates were transferred to a six-well plate (Thermo Fisher Scientific, Waltham, MA, USA).

MSC preparation and labeling
Mouse-derived MSCs (from Balb/C mice) were prepared as previously described.[24] The femurs and tibias of 4- to 6-week-old mice were first flushed with PBS (HyClone) to collect the bone marrow cells. After second passage, the cells were used for subsequent experiments. Finally, the cells were identified by the presence of surface markers through flow cytometry (Becton Dickinson Inc., Franklin Lakes, NJ, USA) as previously described[25] (positive for Sca-1, CD105, CD90 and negative for CD45, CD34, CD31). In the next step, the obtained inverse opal substrates were placed in the incubator (Hera cell 150; Thermo Fisher Scientific) at 37°C and 5% CO_2. After 3 days, the morphology and alignment of the cells on the substrate were observed. For detailed observation of the morphology and alignment, MSCs were further stained with calcein-AM and DAPI and then detected by a fluorescence microscope (Olympus IX71; Olympus Corporation, Tokyo, Japan).

We observed the direction of MSCs grown on the inverse opal substrates at a high magnification of 400×. Expanded direction of the inverse opal substrates represents 0°, growths direction of the spindle shaped MSCs defined as the direction departing from the inverse opal substrates. Then the angle is defined as the certain orientation angle of growing MSCs. The inverse opal substrates (1×1 mm) with loaded MSCs (10^3–10^4 counts) were further used for transplantation after AMI (Figure S2).

Cytotoxicity evaluation

The toxicity of the inverse opal substrates to MSCs was determined through an MTT assay kit. Briefly, after being incubated with inverse opal substrates for 48 hours, MSCs were washed with PBS and 10 µL of MTT reagent was added. Then, dimethyl sulfoxide (150 µL) was used to dissolve the formazan crystals. Finally, the absorbance was read at 490 nm in a microplate reader.

AMI mouse model

All the animal experiments performed in this study were approved by the Institutional Animal Care and Use Committee (IACUC) of Southeast University. All procedures followed were in accordance with the ethical standards of the responsible committee on animal experimentation (institutional and national) and with the Helsinki Declaration of 1964, and the applicable revisions in 1975. All procedures on mice were done in compliance with National Institutes of Health and IACUC guidelines. Balb/c mice were fed regular diet and placed in a dedicated room (25°C–28°C) for small animals as outlined by IACUC of Southeast University.

AMI mice were induced by direct ligation of the left anterior descending artery. Male mice (6–8 weeks old) weighing 20–25 g were used in the experiment (n=12 in each group). After being anesthetized (0.1% pentobarbital sodium [50 mg/kg]) and under ventilator-assisted breathing (110 breaths/minute; Harvard Apparatus), about 1 cm wound layer was cut along the 3–4 intercostal space of the left chest. After the separation of the pericardium, the left side branch of coronary artery was ligated with an 8–0 nylon suture below the left auricular level. Three unipolar limb leads (left upper limb and two lower limbs) associated ST elevation was considered to be a successful AMI model.

Cell viability and secretion determination

After digestion with 0.25% trypsin with EDTA and further washing with PBS, MSCs were collected. The mitochondrial membrane potential of the cultured MSCs in the two-dimensional plane and in the inverse opal substrates was determined using the FACSCalibur cytometer with JC-1 mitochondrial membrane potential assay kits (Abnova).

For flow cytometry test, isolated MSCs were stained with tetraethylbenzimidazolylcarbocyanine iodide (JC-1) according to the standard protocol.[26] After incubation for 3 hours, to remove suspended suspicious apoptotic cells, fluorescence-activated cell sorter analysis was performed using a FACSCalibur flow cytometer (Becton Dickinson) and FlowJo software version 10.0.6 (Tree Star). About 6,000 events were collected for each sample.

Then, the secretion of growth factors including VEGF-α, Ang-1, and SDF-1 by MSCs in the two groups was determined by mice ELISA kits (R&D Systems Inc.). To further determine the superiority of cells grown on the inverse opal substrates, their membrane potential and ability to secrete growth factors were also detected under hypoxic conditions (99.9% pure nitrogen for 6 hours in a hypoxia box).

Statistical analysis

SPSS 19.0 was used for data analysis and comparison between groups in the experiment. Depending on the expression and distribution of data, Independent *t*-test (for normally distributed data and continuous data) and chi-squared test or Fisher's exact test (for categorical variable data) were used. Kaplan–Meier survival curves were used to compare the death event of mice between groups. All the results in the experiment were considered to be statistically significant when the two-sided *P*-value was ≤0.05.

Results

Characterization of inverse opal substrates

Our inverse opal substrates were first produced through the vertical deposition method. The substrates were further derived from a colloidal crystal template (Figure 1A). To obtain an increased expansion ratio, the film of inverse opal substrates was first heated at 80°C in water and then was stretched to different degrees, which was determined by a Vernier caliper. Structural features of the expanded inverse opal substrates under a scanning electron microscope are shown in Figure 1B. As previously described,[20] pore shape index (PSI $=4\pi A/P^2$, where A is the area and P is the perimeter of the micropores) was used here to determine the association between micropore stretch and micropore morphology. We found the value gradually reduced from 0.93±0.10 (when unexpanded) to 0.74±0.08, 0.40±0.06, and 0.24±0.05 when the expansion ratio was increased by two, four, and six ×, respectively (Figure 1C).
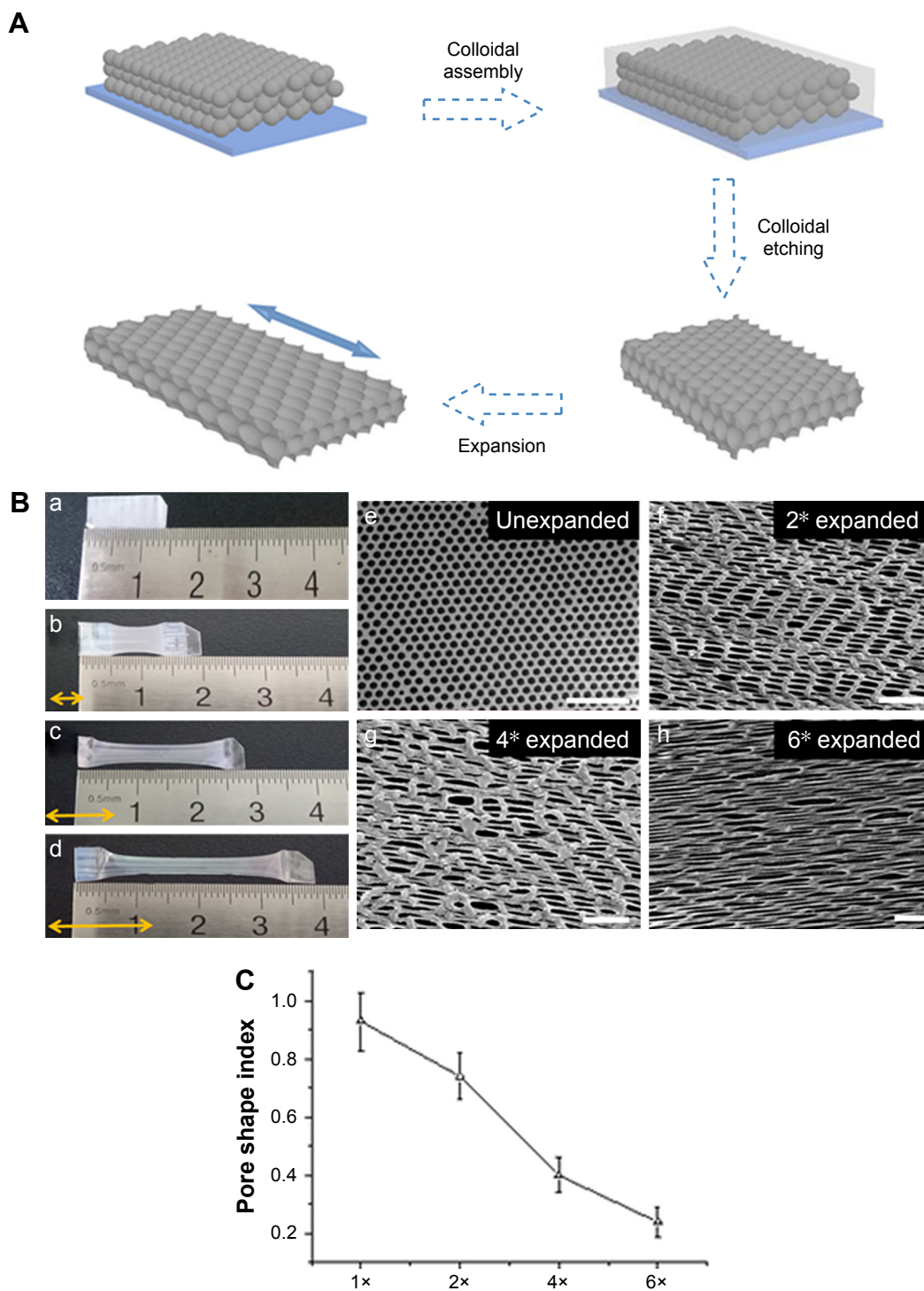
Figure I Characterization of inverse opal substrates.

Notes: (**A**) Schematic diagram of the preparation of the expanded inverse opal substrate. (**B**) Photos and SEM images of SiO_2, inverse opal scaffold expanded by 1–6 times (a–d) and the corresponding pattern on SEM (e–h). The double-sided arrows indicate the direction of expansion. Scale bars in SEM images are 2 μm. (**C**) PSI value calculation, where A is the area and P is the perimeter of the micropores. Usually, the PSI ranges from 1 (a perfect circle) to 0 (a straight line), which reveals the degree of elongation of a nanoscale pore.

Abbreviations: SEM, scanning electron microscopy; PSI, pore shape index.

Biocompatibility of MSCs and inverse opal substrates

We next evaluated the biosafety of this nanomaterial toward MSCs in vitro. MSCs obtained from Balb/c mice were further

seeded into the expanded inverse opal substrates at different time intervals for up to 48 hours, and the cell viability of MSCs was then determined using the MTT assay kit. The results demonstrated that this nanomaterial of inverse opal

substrates is almost relatively nontoxic (P=nonsignificant [NS]) to these MSCs (Figure 2) as compared to the cells growing in a two-dimensional flask.

The novel expanded inverse opal substrate allows orderly growth of MSCs

To confirm the function of the gradient-expanded inverse opal substrate on stem cells, mouse-derived MSCs were seeded on the substrates to mimic the gradient structural organization of cell-to-cell insertion. Owing to the anisotropic behavior of the cells, and with the aim of providing better biological characteristics and functions after MSCs transplantation in vivo, the expanded inverse opal films were treated with O_2 plasma to increase their hydrophilic properties and encourage cell adhesion. The schematic and light microscope images of MSCs on the expanded inverse opal substrates are shown in Figure 3A. Fluorescent images of the MSCs stained with calcein-AM and DAPI are also shown (Figure 3B). As further shown in Figure 3C, the orientation of MSCs on six × (76%±14.5%) expanded substrate was much higher than that

on four (34%±10.6%) and two (20%±7.2%) times expanded as well as unexpanded substrate (13%±4.1%) (P<0.001).

The novel expanded inverse opal substrate provides a certain orientation angle for growing MSCs

To examine the growth orientation of MSCs in response to the differently expanded substrates, we further analyzed the angle of the directional MSCs and the expanding direction. An angle of 0° represents expanding orientation parallel to the substrate, which denotes the long axis of MSC growth. An angle of 90° represents an orientation perpendicular to the radial direction (Figure 4A). As further shown in Figure 4B–E, we found that nearly 90% of MSCs showed orientation angle intervals of less than 30° at 6× expansion (89.6%±5%) compared to the percentage of cells that showed 30°–60° (8.7%±2.6%) or ≥60° (1.7%±1.0%) orientation angle (P<0.001). However, there are still differences in the percentage of the MSCs at 4× stretching (76.3%±25.9% vs 14.7%±4.7% vs 9.0%±3.5% at ≤30°, 30°–60°, ≥60°,
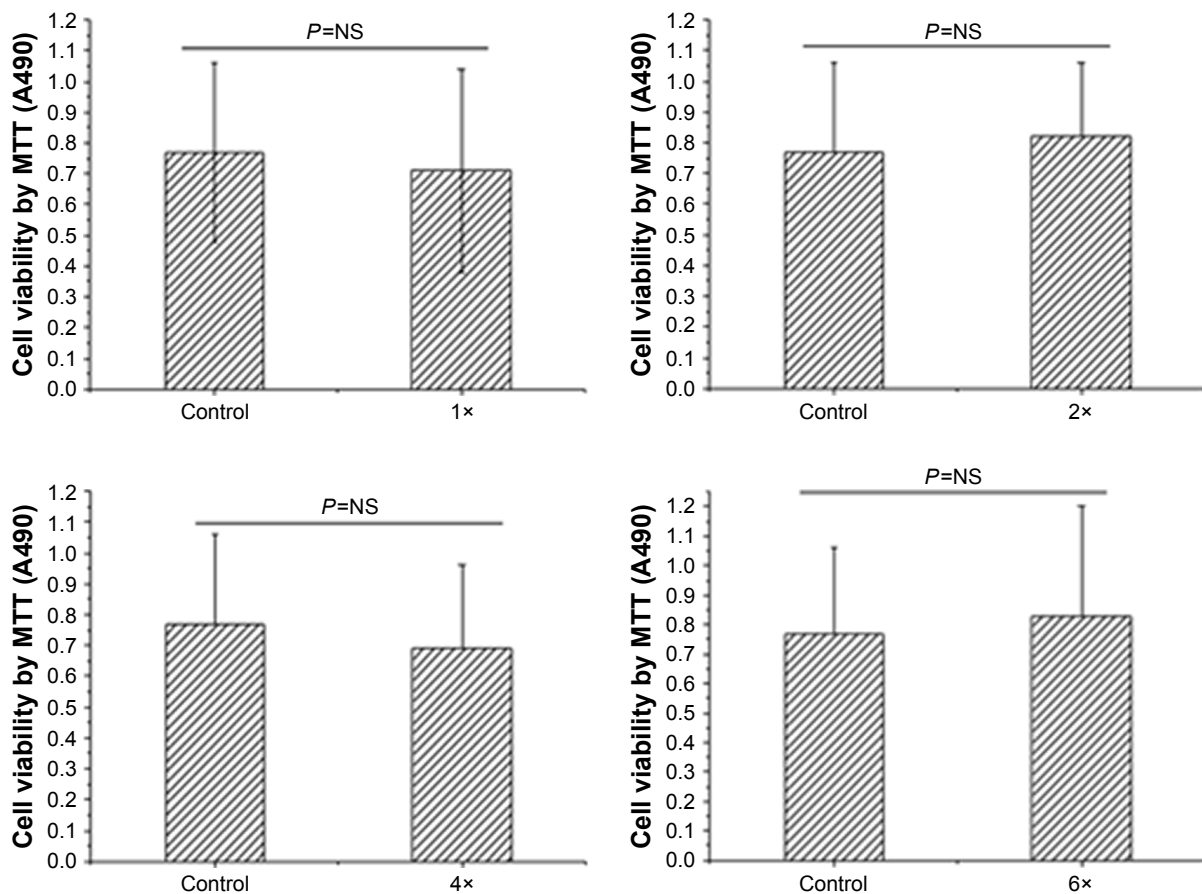
Figure 2 MTT assays of MSCs cultured on different expanded inverse opal substrates.
Note: Control 0.77±0.29/OD490 nm vs 1×, 0.71±0.33/OD490 nm vs 2×, 0.82±0.24/OD490 nm vs 4×, 0.69±0.27/OD490 nm vs 6×, 0.83±0.37/OD490 nm.
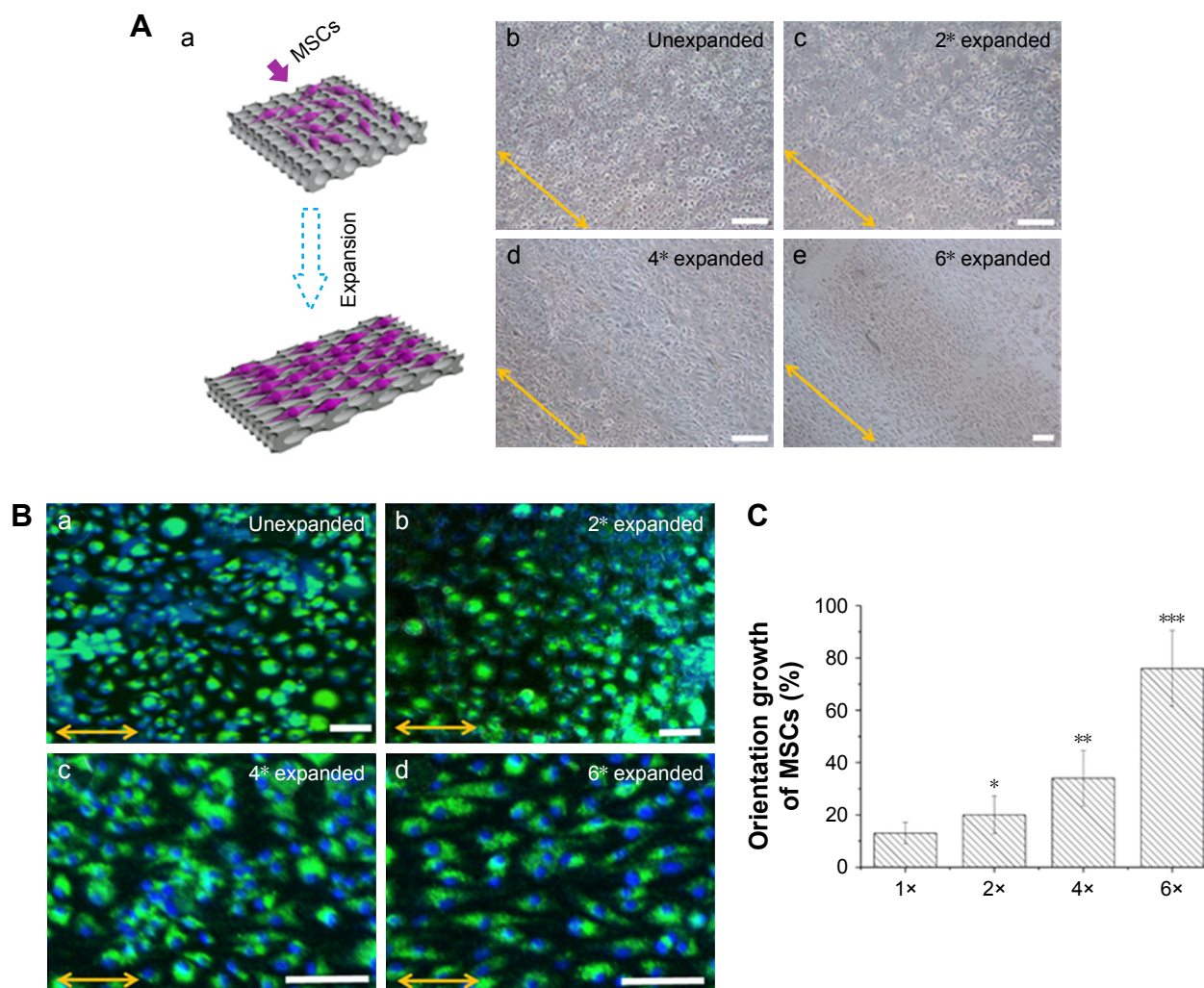**Abbreviation:** MSC, mesenchymal stem cell.

Figure 3 The novel expanded inverse opal subtrate allows orderly growth of MSCs.
Notes: (**A**) Light microscopy images of MSCs. Schemes of MSCs cultured on a gradient-expanded inverse opal substrate (a); light microscopy images of MSCs cultured on different expanded inverse opal substrates (b–e). (**B**) Fluorescence microscopy images of MSCs cultured on a gradient-expanded inverse opal substrate from unexpanded portion to six × of expanded portion (a–d); the double-sided arrows indicate the direction of expansion. Scale bar =200 μm. (**C**) Orientation angle frequency distribution of MSCs cultured on different portions of the expanded inverse opal substrate after 7 days. *$P<0.05$ vs the corresponding control group,** vs 1× and 2×, *** vs 1×, 2× and 4×.
Abbreviation: MSCs, mesenchymal stem cells.

$P<0.001$) and 2× stretching (58%±15.5% vs 37.6%±9.9% vs 4.4%±2.1% at ≤30°, 30°–60°, ≥60°, $P<0.001$). Then the MSCs with orientation angle intervals less than 30° were further compared at 2×, 4×, and 6× times stretching. As shown in Figure S3, significantly more MSCs with orientation angle intervals of less than 30° were observed at 6× than those at 2× and 4× stretching ($P<0.001$). In conclusion, these data demonstrated that due to the higher expansion ratio of the inverse opal substrate, higher percentage of cells grew within 30° angle and were aligned to the expanding direction of the inverse opal substrate. Therefore, further experiments and tests are mainly based on the six × expanded substrate of inverse opal.

Inverse opal-loaded MSC transplantation contributes to decreased apoptosis and LV remodeling

To further determine whether the stereoscopic orientation of cultured MSCs can ameliorate cardiac function after AMI, inverse opal-loaded MSCs were transplanted into AMI mice, as shown in Figure S2. Survival functions at 60 days were first compared (Figure S4), though no statistically significant difference was observed ($P=0.37$), which may be related to a very small sample size. Results showed that survival rate in the control group was lower than that of the inverse opal-loaded MSC transplantation group. We next detected the number of apoptotic cardiomyocytes after 3
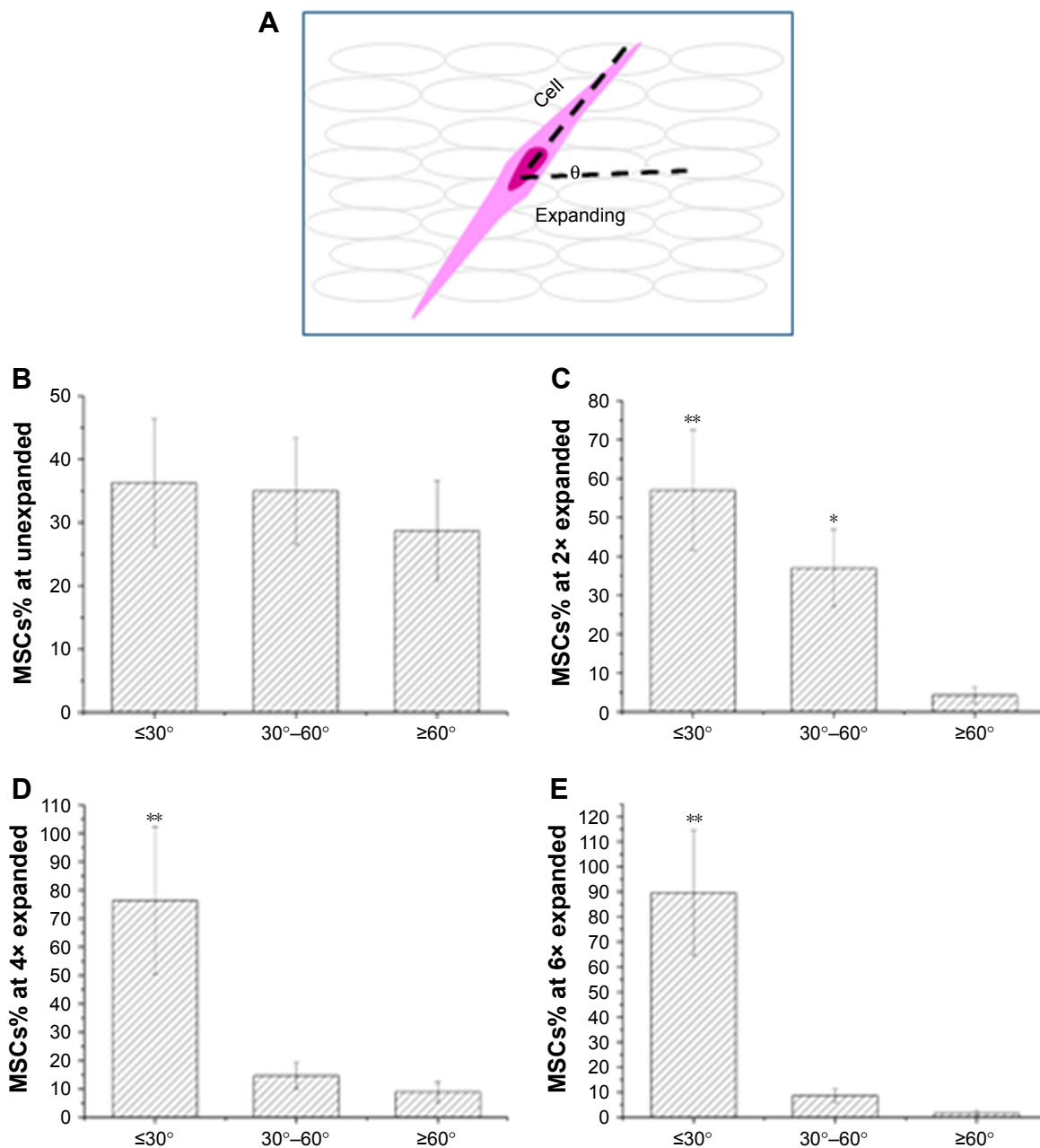
Figure 4 Expanded inverse opal makes a certain orientation angle with growing MSCs.
Notes: (**A**) Schematic diagram of the orientation angle of the cells and the expanded scaffolds. (**B–E**) Percentage of orientated MSCs was calculated at 1×, 2×, 4× and 6× respectively, 500 cells in total were measured on each portion. *$P<0.05$ vs the corresponding control group of $\geq60°$, **$P<0.05$ vs the corresponding control group of both $\geq60°$ and $30°–60°$.
Abbreviation: MSCs, mesenchymal stem cells.

days of transplantation, and as expected, TUNEL[+] cardiac myocytes ($20.45\%\pm8.64\%$ vs $39.63\%\pm11.71\%$, $P<0.001$) in the infarct area decreased greatly as compared to that in the control group 3 days after AMI (Figure 5A and B). Consistent with the decreased apoptotic cardiomyocytes, a significant decrease of left ventricular (LV) remodeling identified by myocardial infarct size at the 14th day (5.87 ± 2.18 mm^2 vs 9.31 ± 3.11 mm^2, $P<0.001$) and the thickness of left ventricular posterior wall at the 21st day (0.93 ± 0.28 mm vs 0.60 ± 0.21 mm, $P<0.001$) was observed after inverse opal-loaded MSC transplantation (Figure 5C–E). Both these results demonstrated that stereoscopic orientation of the cultured MSCs, based on inverse opal, played a promising role post AMI.
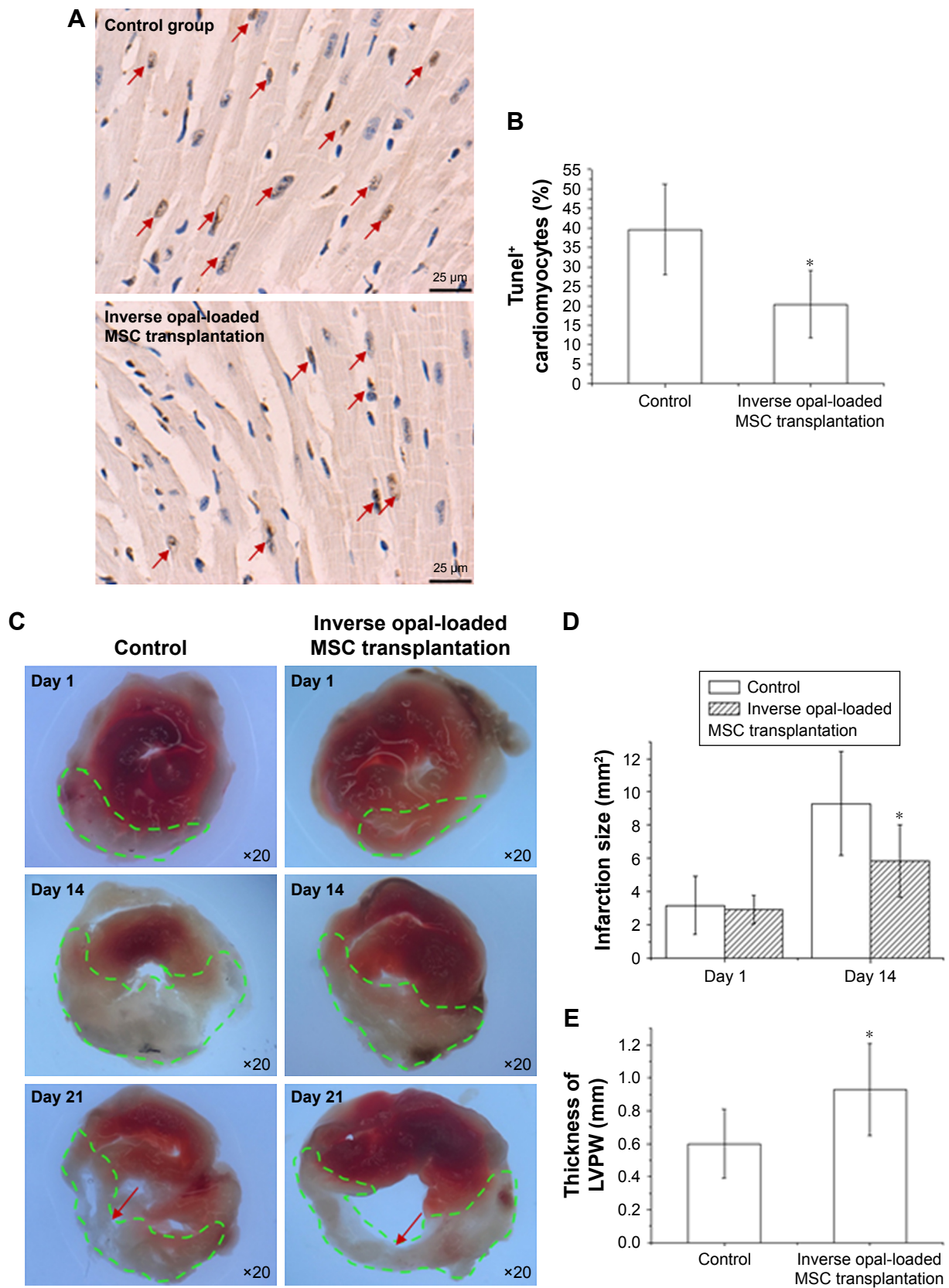
Figure 5 Inverse opal-loaded MSC transplantation contributes to decreased apoptosis and attenuated myocardial remodeling (n=12).
Notes: (**A**, **B**) Image of immunofluorescent staining for TUNEL (apoptotic cardiomyocyte) in the infarct border zone 3 days after MSCs transplantation was shown and compared. (**C–E**) Infarct size at baseline (day 1) and at day 14 as well as the thickness of the LV posterior walls at day 21 in the two groups. The red arrows point to the LVPW at day 21 and the green dashs point to the infarct size. The data represent the mean ± SD. *$P<0.05$ vs the corresponding control group.
Abbreviations: MSCs, mesenchymal stem cells; LVPW, left ventricular posterior wall.

MSCs cultured on inverse opal substrates showed higher viability and increased secretion of growth factors

It is well known that paracrine secretion of growth factors by MSCs, such as VEGF-α, SDF-1, and Ang-1, played an important role in AMI after transplantation.[27] To investigate whether this is the main mechanism by which they exhibit superior therapeutic effect, we next determined the secretion of growth factors by MSCs. As shown in Figure 6A–C, we found that secretion of SDF-1 (17.8 ± 5.9 vs 9.9 ± 3.2 pg/mL, $P<0.001$) and Ang-1 (289.5 ± 54.4 vs 193.5 ± 40.6 pg/mL, $P<0.001$) derived from MSCs that were grown on the 6× expanded inverse opal substrates was extremely higher than that of the unexpanded inverse opal (control group). We further observed that under hypoxic conditions, Ang-1 (228.9 ± 41.7 vs 161.2 ± 30.6 pg/mL, $P<0.001$) and VEGF-α (79.9 ± 26.0 vs 40.8 ± 15.6 pg/mL, $P<0.001$) secreted by MSCs on the substrate were still significantly higher than those

of the corresponding control, which directly indicated that MSCs grown on expanded inverse opal substrate exhibited higher hypoxic tolerance. The mitochondrial membrane potential of the cultured MSCs in the two groups was further determined (2.98 ± 1.03 vs 5.46 ± 1.77, $P<0.001$) at normal conditions and (0.62 ± 0.26 vs $0.91\%\pm0.35\%$, $P<0.001$) under hypoxic conditions (Figure 6D and E). Consistent with the results produced by ELISA, our findings again revealed a significantly higher viability of the cells in the 6× expanded inverse opal group than that in the control group.

Discussion

Recently, many researchers have been actively trying to use MSCs as stem cells for treating AMI.[28,29] Paracrine activity of MSCs was considered to be the main mechanism in mediating the molecular network within the infarct area for heart regeneration.[30,31] However, it has been identified that the transplanted MSCs cannot survive effectively in the host
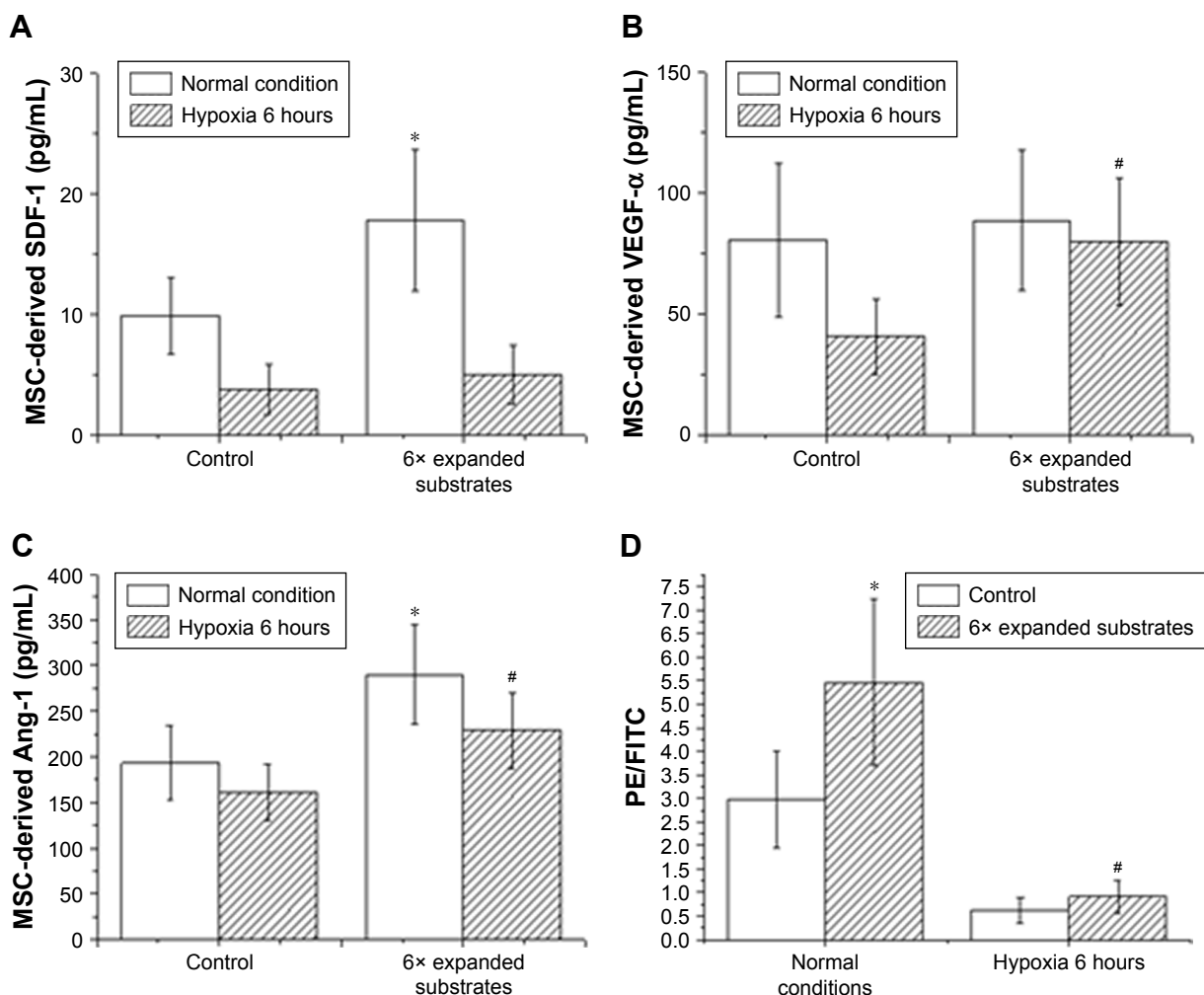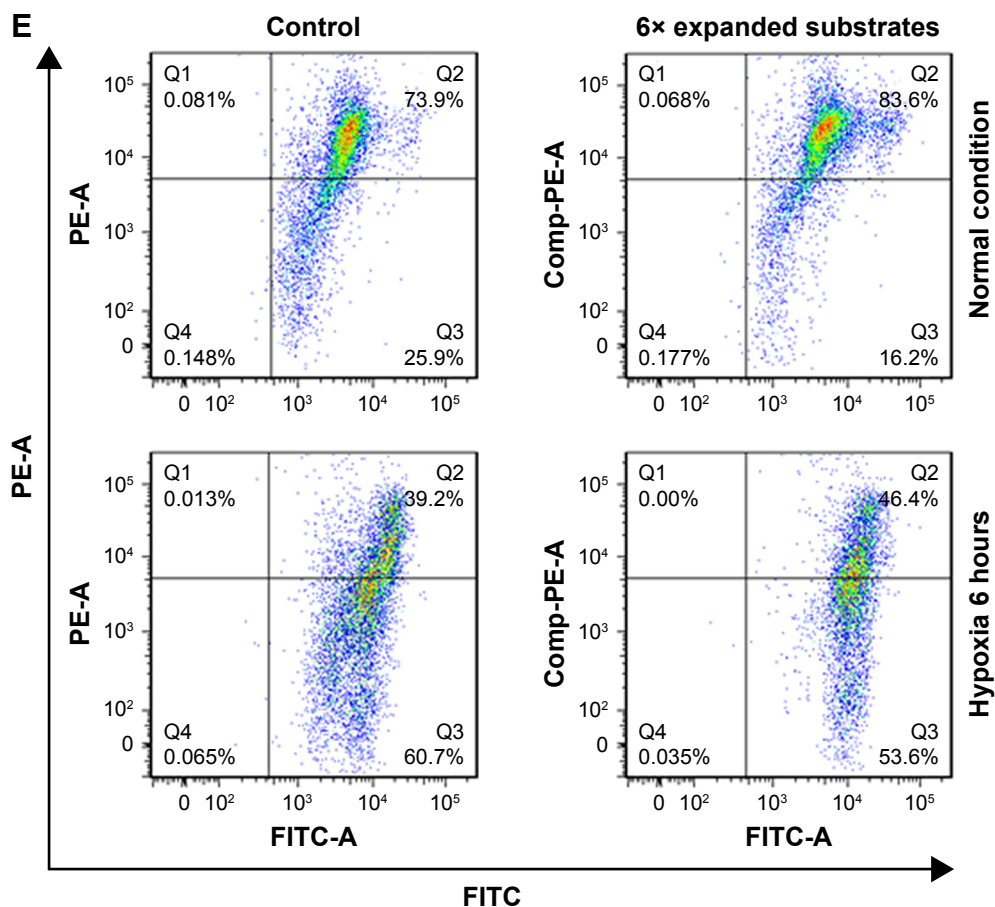

Figure 6 (*Continued*)

Figure 6 Secretion of growth factors by MSCs and cell viability analysis.
Notes: (**A–C**) SDF-1, VEGF-α, and Ang-1 derived from MSCs grown on the substrates of 6× expanded inverse opal (substrates) or unexpanded substrates (control group) were analyzed by ELISA kits. (**D**) Mitochondrial membrane potential of MSCs (calculated by PE/FITC) on the 6× expanded substrates and the control group under normal and hypoxia conditions. (**E**) Representative test results shown by FACSCalibur cytometer analysis. *$P<0.05$ vs the corresponding control group in normal conditions; #$P<0.05$ vs the corresponding control group in hypoxic conditions.
Abbreviations: Ang-1, angiopoietin-1; FITC, fluorescein isothiocyanate; MSCs, mesenchymal stem cells; PE, phycoerythrin; SDF-1, stromal cell-derived factor 1; VEGF-α, vascular endothelium growth factor-α.

due to acute inflammation. Methods to reduce the rate of apoptosis of the transplanted MSCs are urgently needed to enable MSCs to fully exert their stem cell treatment effects.[32] The combined use of cells and nanomaterials has become a consecutive promising trend in cell-based therapies,[33] since increasingly more evidence indicates that new nanomaterials could be generated to provide a relatively better and stable microenvironment for the behavior of stem cells.[34]

The expanded inverse opal substrates used in our experiments were derived from colloidal crystal templates. This gradient-expanded inverse opal substrates displayed a gradual increase in the degree of porous orientation on their surfaces along the direction of expanding. The present study demonstrated that 1) the expanded inverse opal substrates used as a support for MSC growth were not only nontoxic to MSCs but could also regulate the growth of the cells; 2) based on the composition of the 6× expanded inverse opal substrates, the growth of MSCs can be controlled in three dimensions,

including longitudinal growth, change of angle, and density adjustment; 3) marked amelioration in the outcome of AMI mice after inverse opal substrate-based MSC transplantation was observed, as evidenced by the decreased apoptosis of cardiomyocytes at 3 days and decreased LV remodeling at 14 and 21 days after transplantation; 4) marked improvements in MSC viability and secretions were observed under the support of inverse opal substrates, as evidenced by the increased secretion under normal and hypoxic conditions, as well as the amelioration of mitochondrial membrane potential. The above-mentioned features, to a great extent, explain the mechanism of superior therapeutic effect exhibited by inverse opal substrate-based MSC transplantation.

In recent years, increasingly more attention has been paid to three-dimensional cell culture technology.[35,36] At present, there are mainly microcarriers, magnetic suspensions, hanging drop plates, and magnetic three-dimensional bioprinting technologies. However, these culturing technologies still face

some problems:[20,37–41] 1) poor hydrophilicity and the weak ability of cell attachment; 2) result in aseptic inflammation, while polymer degradation easily leads to a drop in local pH; 3) insufficient mechanical strength; and 4) cytotoxicity exhibited by the residues of organic solvents, which may cause fibrosis and immune response to the surrounding and other tissues. In contrast to these traditional substrates, in this study we used expanded inverse opal substrates that provide more opportunities for on-demand stem cell culturing and pave the way for the development of simple treatments for challenging stem cell transplantation. Expanded inverse opal substrates can form a three-dimensional structure,[42,43] which is similar to the physiological morphology of living tissues, and also has high shear sensitivity, which contributes to it being freely switched between solid and liquid phases. The versatility, nontoxicity, biocompatibility, biodegradability, and high biological activity are also beneficial features. In addition, the acceptable stability of expanded inverse opal substrates ensure resistance to mechanical stress and harsh pH conditions in vivo, which are also the most important barriers encountered in vivo for stem cell transplantation. Furthermore, high permeability of the substrates can easily enable immunohistochemical staining, and the subsequent noninvasive monitoring of MSC growth.

Here, the expanded inverse opal substrate-based MSC displayed a controllable alignment along the direction of the stretched gradient of this novel nanomaterial. We observed a concomitant increase in the alignment of cells with the increasing expansion ratio of the substrate. This random-to-aligned cell gradient played a key role in cell growth with subsequent effect on their functions. MSCs are especially known for their secretion of paracrine factors, which have beneficial effects on angiogenesis, cell survival, and restraining inflammation.[25,41,44,45] The encouraging results of opal substrate-based MSC transplantation on AMI mice in this study, as identified by decreased apoptosis of cardiomyocytes and a significant decrease of LV remodeling, are mainly due to this novel method. The secretion effects of MSCs were extremely encouraging, as shown by increased levels of SDF-1, Ang-1, and VEGF-α. These data directly demonstrated that the culture on this substrate were superior to the conventional culture. This advantage is also obvious under hypoxic conditions, which indicates that hypoxia tolerance of MSCs grown on the expanded inverse opal substrates is much better than that exhibited by the common culture.

Notably, the current therapeutic effects of stem cells for AMI are mostly based on the effective survival of the cells. The current challenge for the application of stem cell transplantation in vivo is the development of an efficient and nontoxic delivery vector. Here, we not only successfully cultured stem cells (MSCs) on inverse opal substrates for the first time but also found that the stem cells maintained high activity on the surface of the carrier. It is worth noting that these are two very crucial points in MSC transplantation after myocardial infarction, and we did observe decreased apoptosis of cardiac myocytes and infarct area in the heart of AMI mice after transplantation.

Conclusion

In summary, we demonstrated that the nanomaterials of inverse opal structures with different orientations can be produced and expanded. Methods to create random-to-aligned oriented morphologies of MSCs were determined. The most prominent is the use of inverse opal substrate loaded MSCs that greatly benefited the injured heart recovery in AMI mice. We further identified the mechanisms underlying the therapeutic effect of this inverse opal substrate-based MSCs therapy, and found that cells present on the substrates showed relatively good viability and increased secretions despite being in hypoxic conditions and under the condition of AMI.

Future perspective

The structure of inverse opal can not only adjust the arrangement of MSCs but can also contribute to its orientated growth. Inverse opal-loaded MSC transplantation extremely curbed myocardial remodeling; the underlying mechanisms might be due to the high viability and increased secretion of growth factors by MSCs, as evidenced by this method. These features of the functional expanded inverse opal substrates with MSCs provide great promise for their clinical use in myocardial infarction.

Acknowledgment

Disclosure

The authors report no conflicts of interest in this work.

References

1. Micheu MM, Dorobantu M. Fifteen years of bone marrow mononuclear cell therapy in acute myocardial infarction. *World J Stem Cells*. 2017;9(4):68–76.
2. van der Laan AM, Ter Horst EN, Delewi R, et al. Monocyte subset accumulation in the human heart following acute myocardial infarction and the role of the spleen as monocyte reservoir. *Eur Heart J*. 2014; 35(6):376–385.
3. Hofer HR, Tuan RS. Secreted trophic factors of mesenchymal stem cells support neurovascular and musculoskeletal therapies. *Stem Cell Res Ther*. 2016;7(1):131.

4. Mestas J, Ley K. Monocyte-endothelial cell interactions in the development of atherosclerosis. *Trends Cardiovasc Med*. 2008;18(6): 228–232.

5. Yuan Y, Du W, Liu J, et al. Stem Cell-Derived Exosome in Cardiovascular Diseases: Macro Roles of Micro Particles. *Front Pharmacol*. 2018;9:547.

6. van den Akker F, de Jager SC, Sluijter JP. Mesenchymal stem cell therapy for cardiac inflammation: immunomodulatory properties and the influence of toll-like receptors. *Mediators Inflamm*. 2013;2013: 181020.

7. Maranda EL, Rodriguez-Menocal L, Badiavas EV. Role of Mesenchymal Stem Cells in Dermal Repair in Burns and Diabetic Wounds. *Curr Stem Cell Res Ther*. 2017;12(1):61–70.

8. Yannas IV. Emerging rules for inducing organ regeneration. *Biomaterials*. 2013;34(2):321–330.

9. Zhao Y, Cheng Y, Shang L, Wang J, Xie Z, Gu Z. Microfluidic synthesis of barcode particles for multiplex assays. *Small*. 2015;11(2): 151–174.

10. Li Y, Wang S, Huang R, et al. Evaluation of the effect of the structure of bacterial cellulose on full thickness skin wound repair on a microfluidic chip. *Biomacromolecules*. 2015;16(3):780–789.

11. Dangi AK, Sharma B, Khangwal I, Shukla P. Combinatorial Interactions of Biotic and Abiotic Stresses in Plants and Their Molecular Mechanisms: Systems Biology Approach. *Mol Biotechnol*. 2018;60(8): 636–650.

12. Cheng Y, Zheng F, Lu J, et al. Bioinspired multicompartmental microfibers from microfluidics. *Adv Mater*. 2014;26(30):5184–5190.

13. Xie J, Li X, Lipner J, et al. "Aligned-to-random" nanofiber scaffolds for mimicking the structure of the tendon-to-bone insertion site. *Nanoscale*. 2010;2(6):923–926.

14. Yan S, Xia P, Xu S, et al. Nanocomposite Porous Microcarriers Based on Strontium-Substituted HA-g-Poly(γ-benzyl-l-glutamate) for Bone Tissue Engineering. *ACS Appl Mater Interfaces*. 2018;10(19): 16270–16281.

15. Han Y, Lu Z, Teng Z, et al. Unraveling the Growth Mechanism of Silica Particles in the Stöber Method: In Situ Seeded Growth Model. *Langmuir*. 2017;33(23):5879–5890.

16. Lee WS, Kang T, Kim SH, Jeong J. An Antibody-Immobilized Silica Inverse Opal Nanostructure for Label-Free Optical Biosensors. *Sensors*. 2018;18(1):E307:307.

17. Lu J, Zou X, Zhao Z, Mu Z, Zhao Y, Gu Z. Cell orientation gradients on an inverse opal substrate. *ACS Appl Mater Interfaces*. 2015;7(19): 10091–10095.

18. Lu J, Zheng F, Cheng Y, Ding H, Zhao Y, Gu Z. Hybrid inverse opals for regulating cell adhesion and orientation. *Nanoscale*. 2014;6(18): 10650–10656.

19. Zhu YX, Jia HR, Pan GY, Ulrich NW, Chen Z, Wu FG. Development of a Light-Controlled Nanoplatform for Direct Nuclear Delivery of Molecular and Nanoscale Materials. *J Am Chem Soc*. 2018;140(11): 4062–4070.

20. Fu F, Chen Z, Zhao Z, et al. Bio-inspired self-healing structural color hydrogel. *Proc Natl Acad Sci U S A*. 2017;114(23):5900–5905.

21. Chen Z, Mo M, Fu F, et al. Antibacterial Structural Color Hydrogels. *ACS Appl Mater Interfaces*. 2017;9(44):38901–38907.

22. Ge H, Wang G, He Y, et al. Photoswitched wettability on inverse opal modified by a self-assembled azobenzene monolayer. *Chemphyschem*. 2006;7(3):575–578.

23. Zhang P, Zhang F, Zhao C, Wang S, Liu M, Jiang L. Superspreading on Immersed Gel Surfaces for the Confined Synthesis of Thin Polymer Films. *Angew Chem Int Ed Engl*. 2016;55(11):3615–3619.

24. Pedersen TO, Blois AL, Xue Y, et al. Mesenchymal stem cells induce endothelial cell quiescence and promote capillary formation. *Stem Cell Res Ther*. 2014;5(1):23.

25. Lu W, Fu C, Song L, et al. Exposure to supernatants of macrophages that phagocytized dead mesenchymal stem cells improves hypoxic cardiomyocytes survival. *Int J Cardiol*. 2013;165(2):333–340.

26. Yokosuka T, Goto H, Fujii H, et al. Flow cytometric chemosensitivity assay using JC-1, a sensor of mitochondrial transmembrane potential, in acute leukemia. *Cancer Chemother Pharmacol*. 2013;72(6): 1335–1342.

27. Zhao Z, Wang J, Lu J, et al. Tubular inverse opal scaffolds for biomimetic vessels. *Nanoscale*. 2016;8(28):13574–13580.

28. Ale A, Siebenhaar F, Kosanke K, et al. Cardioprotective C-kit⁺ bone marrow cells attenuate apoptosis after acute myocardial infarction in mice – in-vivo assessment with fluorescence molecular imaging. *Theranostics*. 2013;3(11):903–913.

29. Ieda M. Heart regeneration using reprogramming technology. *Proc Jpn Acad Ser B Phys Biol Sci*. 2013;89(3):118–128.

30. Raicevic G, Najar M, Najimi M, et al. Influence of inflammation on the immunological profile of adult-derived human liver mesenchymal stromal cells and stellate cells. *Cytotherapy*. 2015;17(2):174–185.

31. Sesia SB, Duhr R, Medeiros da Cunha C, et al. Anti-inflammatory/tissue repair macrophages enhance the cartilage-forming capacity of human bone marrow-derived mesenchymal stromal cells. *J Cell Physiol*. 2015;230(6):1258–1269.

32. Liu B, Duan CY, Luo CF, et al. Impact of Timing following Acute Myocardial Infarction on Efficacy and Safety of Bone Marrow Stem Cells Therapy: A Network Meta-Analysis. *Stem Cells Int*. 2016;2016: 1031794–11.

33. Su N, Gao PL, Wang K, Wang JY, Zhong Y, Luo Y. Fibrous scaffolds potentiate the paracrine function of mesenchymal stem cells: A new dimension in cell-material interaction. *Biomaterials*. 2017;141: 74–85.

34. Choi SW, Zhang Y, Xia Y. Three-dimensional scaffolds for tissue engineering: the importance of uniformity in pore size and structure. *Langmuir*. 2010;26(24):19001–19006.

35. Skeldon G, Lucendo-Villarin B, Shu W. Three-dimensional bioprinting of stem-cell derived tissues for human regenerative medicine. *Philos Trans R Soc Lond B Biol Sci*. 2018;373(1750):20170224pii.

36. Yuan H, Xing K, Hsu HY. Trinity of Three-Dimensional (3D) Scaffold, Vibration, and 3D Printing on Cell Culture Application: A Systematic Review and Indicating Future Direction. *Bioengineering (Basel)*. 2018;5(3):pii:E57.

37. Nakamura T, Sato T. Advancing Intestinal Organoid Technology Toward Regenerative Medicine. *Cell Mol Gastroenterol Hepatol*. 2018; 5(1):51–60.

38. Rothbauer M, Zirath H, Ertl P. Recent advances in microfluidic technologies for cell-to-cell interaction studies. *Lab Chip*. 2018;18(2): 249–270.

39. Maartens JH, de-Juan-Pardo E, Wunner FM, et al. Challenges and opportunities in the manufacture and expansion of cells for therapy. *Expert Opin Biol Ther*. 2017;17(10):1221–1233.

40. Ravi M. Applications of Three-Dimensional Cell Cultures in the Early Stages of Drug Discovery, Focusing on Gene Expressions, Drug Metabolism, and Susceptibility. *Crit Rev Eukaryot Gene Expr*. 2017; 27(1):53–62.

41. Zheng Y, Wang G, Chen R, Hua Y, Cai Z. Mesenchymal stem cells in the osteosarcoma microenvironment: their biological properties, influence on tumor growth, and therapeutic implications. *Stem Cell Res Ther*. 2018;9(1):22.

42. Sommer MR, Vetsch JR, Leemann J, Müller R, Studart AR, Hofmann S. Silk fibroin scaffolds with inverse opal structure for bone tissue engineering. *J Biomed Mater Res B Appl Biomater*. 2017;105(7):2074–2084.

43. Kim J, Bencherif SA, Li WA, Mooney DJ. Cell-friendly inverse opal-like hydrogels for a spatially separated co-culture system. *Macromol Rapid Commun*. 2014;35(18):1578–1586.

44. Williams AR, Hare JM. Mesenchymal stem cells: biology, pathophysiology, translational findings, and therapeutic implications for cardiac disease. *Circ Res*. 2011;109(8):923–940.

45. Miyahara Y, Nagaya N, Kataoka M, et al. Monolayered mesenchymal stem cells repair scarred myocardium after myocardial infarction. *Nat Med*. 2006;12(4):459–465.
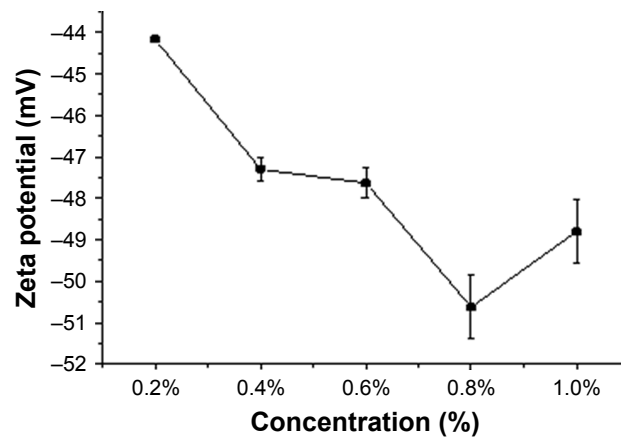
Supplementary materials

Figure S1 The zeta potential of nanoparticles at different concentrations.

Notes: The fabrication of an inverse opal was made of monodisperse silica spheres. To evaluate the effect of nanoparticle concentration on the stability of the inverse opal, a series of nanoparticles at different concentrations (0.20 wt%, 0.40 wt%, 0.60 wt%, 0.80 wt%, and 1 wt%) were tested. At the end, the preparation conditions were determined to be 1.0 wt% for the silica nanoparticle concentration in the experiment.
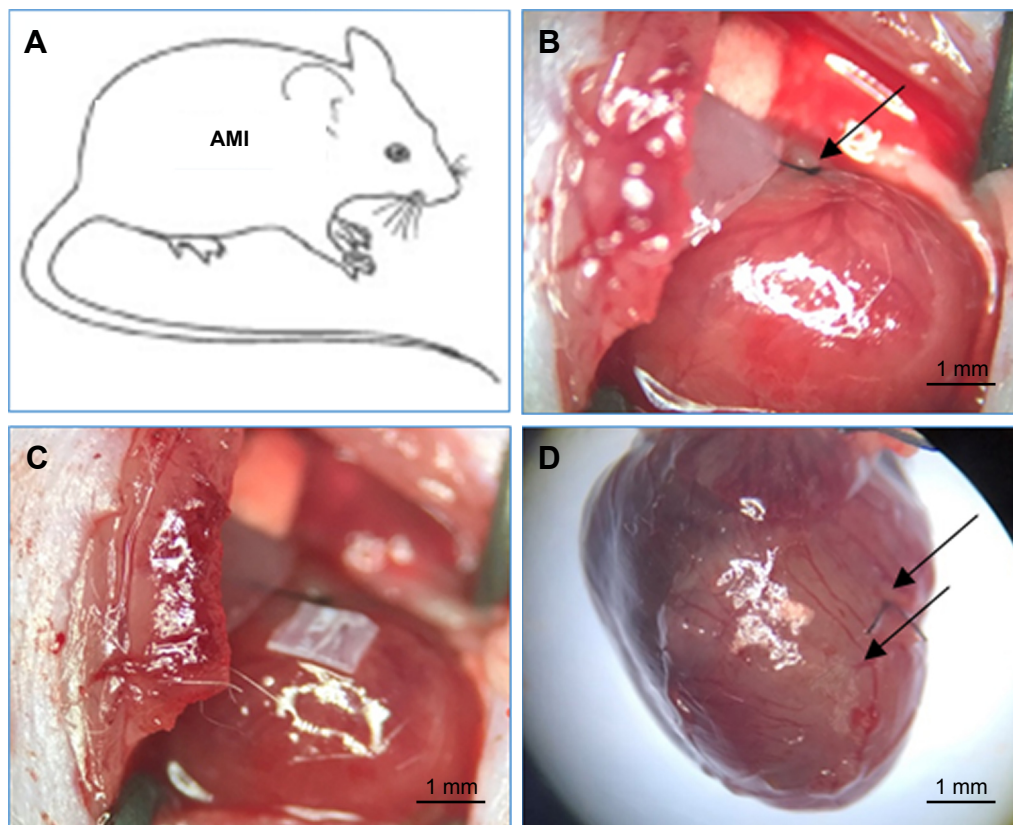
Figure S2 AMI mice coronary vessels was ligated inverse opal-loaded MSC transplantation in vivo.

Notes: (**A**) Illustration for AMI mice; (**B**) ligation of the LAD artery (black arrow); (**C**) inverse opal-loaded MSCs (1×1 mm) transplanted into the heart of AMI mice; and (**D**) after the AMI mice were executed at 14–21 days, the interruption of blood flow and the surrounding infarcted myocardium can be seen (black arrow below).

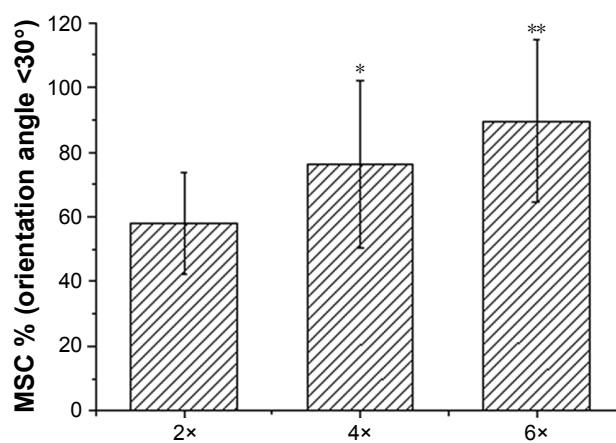**Abbreviations:** AMI, acute myocardial infarction; LAD, left anterior descending; MSCs, mesenchymal stem cells.

Figure S3 The comparison of orientation angle intervals of MSCs <30° at 2×, 4×, and 6× times stretching.
Note: *$P<0.05$ vs the corresponding control group, **of 6× vs. 2× and 4×.
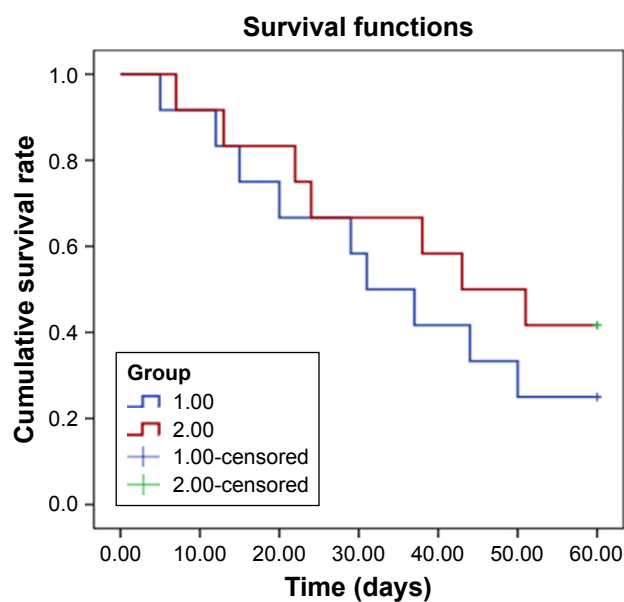**Abbreviation:** MSCs, mesenchymal stem cells.

Figure S4 Survival curves (n=12 in each group) at 60 days showed the survival rate of the control group (blue line) is lower than that of the inverse opal-loaded MSC transplantation group ($P=0.37$), though there was no statistically significant difference (this may be related to a very small sample size).